Cytokinin oxidase/dehydrogenase family genes exhibit functional divergence and overlap in rice growth and development

Chenyu Rong [1], Yuexin Liu [1], Zhongyuan Chang [1], Ziyu Liu [1], Yanfeng Ding [1,2,3] and Chengqiang Ding [1,2,3,*]

[1]College of Agriculture, Nanjing Agricultural University, Nanjing 210095, People's Republic of China

[2]Key Laboratory of Crop Physiology Ecology and Production Management, Ministry of Agriculture, Nanjing 210095, People's Republic of China

[3]Collaborative Innovation Center for Modern Crop Production co-sponsored by Province and Ministry, Nanjing 210095, People's Republic of China

*Correspondence: Chengqiang Ding, email: dingcq@njau.edu.cn. ORCID: 0000-0001-6061-1979

Running title: The important functions of *OsCKX* family genes in rice

Highlight: The *osckx4 osckx9* double mutant had a significantly greater number of tillers, whereas the *osckx1 osckx2* double mutant showed the opposite phenotypic change, compared to the wild type.

ABSTRACT

Cytokinins play key roles in plant growth and development; hence, cytokinin biosynthesis and degradation have been extensively studied. Cytokinin oxidase/dehydrogenases (CKXs) are a group of enzymes that regulate oxidative cleavage to maintain cytokinin homeostasis. In rice, 11 *OsCKX* genes have been identified to date; however, most of their functions remain unknown. Here, we comprehensively analyzed the expression patterns and functions of *OsCKX* genes. Using CRISPR/Cas9 technology, we constructed mutants of all *OsCKX* genes to determine the functions of OsCKXs in rice development. The results revealed that the single *osckx* and higher-order *osckx4 osckx9* mutant lines showed functional overlap and subfunctionalization. Notably, the *osckx1/2* and *osckx4/9* double mutants displayed contrasting phenotypic changes in tiller number, culm diameter, and panicle size compared to the wild type. Moreover, we identified several genes with significantly altered expression in *osckx4* and *osckx9* single and double mutant plants. Many differentially expressed genes were found to be associated with auxin and cytokinin pathways. Additionally, the cytokinins in *osckx4/9* mutants was increased compared to the wild type. Overall, our findings provide new insights into the functions of *OsCKX* genes in rice growth and may be used as a foundation for future studies aimed at improving rice yield.

Key words: Cytokinin, expression pattern, *OsCKX*, panicle, phenotype, rice, tiller

INTRODUCTION

Cytokinin controls plant growth and development by promoting plant cell division, growth, and differentiation. Specifically, it is responsible for stem enlargement and differentiation, organ development and structure, nutrition absorption, senescence, and stress response. Cytokinin biosynthesis starts from the ADP, ATP, or tRNA catalyzed by different adenosine phosphate isopentenyl transferases and activated by LONELY GUY enzymes (Kurakawa *et al.*, 2007; Osugi *et al.*, 2017). After performing its function, cytokinin is inactivated by certain enzymes such as cytokinin oxidase/dehydrogenases (CKXs) that induce cytokinin oxidative cleavage, which is an irreversible process. CKXs are essential for maintaining cytokinin homeostasis during plant growth and development. Therefore, extensive research on CKXs has been conducted and is still ongoing.

Each plant species has a group of *CKX* genes, for example, *Arabidopsis* has seven, rice has 11, and maize has 13. Most CKXs in maize and *Arabidopsis* have putative N-terminal secretory peptides that assist in locating the endoplasmic reticulum (ER) (Niemann *et al.*, 2018; Zalabak *et al.*, 2016). Previous studies have discovered several functions of CKXs in *Arabidopsis* and other crops. In *Arabidopsis*, the overexpression of *AtCKX1* and *AtCKX2* resulted in smaller shoots, larger roots, and smaller shoot apical meristems (SAMs), while *AtCKX7* overexpression resulted in shorter primary roots (Kollmer *et al.*, 2014; Werner *et al.*, 2001). Furthermore, *ckx3 ckx5* mutants developed larger SAM and more siliques (Bartrina *et al.*, 2011). Sextuple *ckx3 ckx5* mutants of oilseed rape showed larger and more active inflorescence meristems (Schwarz *et al.*, 2020). In barley, *HvCKX1* downregulation resulted in more spikes, more grains per spike, and a higher 1,000-grain weight (Zalewski *et al.*, 2010). *TaCKX6-D1* was found to be associated with grain filling and grain size in wheat (Zhang *et al.*, 2012).

In rice, *OsCKX2/Gn1a* was the first *CKX* gene identified. Rice varieties with low *OsCKX2*

expression yielded more grains per panicle, while *OsCKX2* downregulation or *osckx2* mutation produced more tillers, more grains per panicle, and heavier grains (Ashikari *et al.*, 2005; Yeh *et al.*, 2015). *OsCKX4* overexpression reduced the tiller number, grain number per panicle, grain weight, and plant height, while it increased the number of roots (Gao *et al.*, 2014). On the other hand, *osckx9* mutants developed more tillers and smaller panicles, while *OsCKX9* overexpression mutants displayed more tillers, shorter culms, smaller panicles, and lower setting rates (Duan *et al.*, 2019). *OsCKX11* was found to regulate leaf senescence and grain number, while *osckx11* mutation resulted in the increased number of spikelets per panicle and tillers (Zhang *et al.*, 2020).

In rice breeding, *OsCKX2* has been artificially selected from wild rice since ancient times and can be divided into alleles from different geographic distributions (Ashikari *et al.*, 2005; Wang *et al.*, 2015). Since most plants with downregulated *CKX* expression exhibit better phenotypes, researchers believed that *CKX* is a potential target to improve yield or to initiate another "Green Revolution" (Ashikari *et al.*, 2005; Chen *et al.*, 2020; Jameson and Song, 2020). Numerous studies have analyzed the structures of and genetic relationships between *OsCKXs*. However, the expression patterns that may determine their functions during plant growth, especially of *OsCKXs* with similar amino acid sequences, are yet to be elucidated.

OsCKX genes play an important role in the crosstalk between cytokinin and other hormones by regulating cytokinin content in plant tissues. Most *OsCKX* genes are upregulated by exogenous cytokinins, such as *trans*-zeatin (tZ), N^6-(Δ^2-isopentenyl) adenine (iP) and 6-benzylaminopurine (6-BA) (Duan *et al.*, 2019). *OsCKX4* can be induced by auxin, which plays a role in regulating the root system (Gao *et al.*, 2014). In addition, *OsCKX9* acts downstream of strigolactones (SLs) and plays a key role in the crosstalk between cytokinin and SLs. The SL-induced activation of *OsCKX9* relies on D53,

which acts as a repressor of SL signaling and consequently functions in the SL-induced regulation of tiller development (Duan *et al.*, 2019). On the other hand, *OsCKX11* has antagonistic roles between the cytokinin and abscisic acid (ABA) pathways during leaf senescence. In *osckx11* mutants, the downregulation of ABA biosynthesis genes and the upregulation of ABA degradation genes result in the reduction of ABA content in flag leaves and subsequently regulate leaf senescence, which shows the relationship between cytokinin and ABA. Thus, these findings demonstrate that *OsCKX* genes act as bridges between cytokinin and other plant hormones (Zhang *et al.*, 2021).

In this study, we investigated the genetic relationships and expression patterns of *OsCKX* genes using RNA sequencing (RNA-seq). We evaluated the phenotypes of *osckx* single and double mutants produced using CRISPR/Cas9 technology to determine the function of different *OsCKX*s. We also analyzed the transcriptomes of the roots and shoot bases from Nipponbare (NIP), *osckx4*, *osckx9*, and *osckx4/9* mutants to identify the genes that were influenced by *OsCKX4* and *OsCKX9*. Our findings may provide new insights regarding the potential application of *OsCKX* genes for improving agricultural traits.

MATERIALS AND METHODS

Plant materials and growth conditions

Oryza sativa L. ssp. *japonica* (cultivars: NIP and ZH11) was the wild-type (WT) rice material chosen for this study. The mutants included *osckx3*, *osckx4*, *osckx5*, *osckx1/2*, *osckx9*, *osckx4/9*, and *osckx6/7/10* from NIP and *osckx1*, *osckx2*, *osckx7*, *osckx8*, *osckx9*, and *osckx11* from ZH11 (Supplemental Figure S1–S3). The target for *osckx1/2* matches *OsCKX1* and *OsCKX2* completely, and has a 1-bp mismatch for *OsCKX11*. The sequencing results showed that the *osckx1/2-19* and *osckxx1/2-21* line had a 1-bp insertion in *OsCKX1* and *OsCKX2*, respectively, but no change was observed in *OsCKX11* (Supplemental Figure S2A).

The rice plants were grown in a field in Danyang, Jiangsu Province, China (31.907° N 119.466° E). We used 300 kg/hm^2 nitrogen, 150 kg/hm^2 P_2O_5, and 240 kg/hm^2 K_2O as base fertilizers for the field experiment. For the pot experiment, 4.28 g of urea was added to each pot, while 1.92 g of KH_2PO_4 and 1.49 g KCl were used during the whole growth period. For the hydroponic experiment, the nutrient solution was composed of 2 mM KNO_3 and 2 mM NH_4Cl, and the concentrations of other nutrient elements were the same as those described by Wang *et al.*, 2020. The plants were grown in climate chambers under long-day conditions (15 h light at 28 °C and 9 h dark at 24 °C) with a relative humidity of ~70%, and the treatment lasted 20 days.

Plasmid construction for genetic transformation

To construct the mutants for research by using CRISPR/Cas9 technology, as previously described, each *OsCKX* gene was assigned one to two single guide RNA oligo targets by using CRISPR/Cas9 technology as previously described (Mao *et al.*, 2013). The primers used for vector construction and genotyping are shown in Supplemental Table S1.

To construct *pOsCKX::GUS*, an upstream fragment of the *OsCKX*-encoding region (>3 kb) was amplified by PCR, and the resulting amplicon was excised with the corresponding restriction endonuclease and ligated into the *pCAMBIA1300::GUS* vector (Wang *et al*., 2020). The primers used for vector construction are shown in Supplemental Table S1.

Analysis of GUS activity

The GUS reporter activity was assayed by histochemical staining using GUS Staining Kit (FCNCS, https://www.fcncs.com). Various tissues were collected from *pOsCKX::GUS* transgenic plants at each developmental stage. After dipping in the GUS staining solution, the samples were taken out and then incubated in the staining solution for 6–48 h at 37 °C in the dark. The samples were de-stained thrice with 70% ethanol in a water bath for 5 min. Images were taken using SZX16 microscope (Olympus, Tokyo, Japan; https://www.olympus-lifescience.com/en/). Each *pOsCKX::GUS* transgenic plant had 20 independent lines, from which 2 or 3 independent lines were chosen and subjected to staining at the same position as other lines for further studies.

Sampling, RNA extraction, and gene expression analysis

We collected roots from approximately 2 cm under the tip and shoot bases (~5-mm segments from the first nodes) containing the SAM, axillary buds, young leaves, and tiller nodes from the WT, *osckx4*, *osckx9*, and *osckx4/9* plants. The samples were stored at −80 °C until further use.

Total RNA was extracted using an E.Z.N.A.® Plant RNA Kit (Omega Bio-tek Inc., Norcross, GA, USA; https://www.omegabiotek.com/) and subjected to reverse-transcription using a PrimeScript™ RT Reagent Kit (Takara Biotechnology, Tokyo, Japan). Quantitative reverse-transcription PCR was performed on an ABI PRISM 7300 Real-Time PCR System (Applied Biosystems, Thermo Fisher Scientific, Waltham, MA, USA; https://www.thermofisher.com/) with SYBR® Premix Ex Taq™

(Takara), following the manufacturer's instructions. Relative expression analysis was performed using the actin gene as internal control. The primers used are listed in Supplemental Table S1.

Sequence alignment and phylogenetic analysis

The amino acid sequence alignment was performed using MUSCLE (Madeira *et al.*, 2019), and phylogenetic trees were generated using a neighbor-joining method and 1,000 bootstrap iterations in MEGA X (Kumar *et al.*, 2018).

RNA-Seq and data analysis

Before library preparation, oligo (dT)-attached magnetic beads (Invitrogen, Cat. No. 61006) were used to purify the mRNA. An MGIEasy RNA Library preparation kit was used for library construction from purified mRNA according to the manufacturer's instruction (BGI, Cat. No. 1000006383). The quality of the constructed library was checked and sequenced after passing. High-throughput sequencing was paired-end sequenced on the BGISEQ-500 platform (BGI-Shenzhen, China). The obtained reads were processed and analyzed, and genes with Q values of < 0.05 and $\log_2$(fold change) values of > 1 or < -1 were considered to be significantly differentially expressed. Based on the list of DEGs, we created and modified Venn diagrams in Microsoft Excel. Furthermore, we performed KEGG enrichment analysis ($Q < 0.05$) (Kanehisa, 2019), and generated a bubble chart using R.

Sampling and quantification of cytokinins

From the WT and *osckx4/9* plants, we collected roots from approximately 5 cm below the tip and shoot bases (~5-mm segments from the first nodes) containing the SAM, axillary buds, young leaves, and tiller nodes. The samples were stored at −80 °C until further use. Endogenous cytokinin levels were quantified by Webiolotech (Nanjing, China) with the ESI-HPLC-MS/MS method, using isotope internal standard as previously reported (Cai et al., 2013).

ACCESSION NUMBERS

Sequence data from this article can be found in Rice Annotation Project database (http://rice.plantbiology.msu.edu) under the following accession numbers: *Actin* (Os03g0718100), *OsCKX1* (Os01g0187600), *OsCKX2* (Os01g0197700), *OsCKX3* (Os10g0483500), *OsCKX4* (Os01g0940000), *OsCKX5* (Os01g0775400), *OsCKX6* (Os02g0220000), *OsCKX7* (Os02g0220100), *OsCKX8* (Os04g0523500), *OsCKX9* (Os05g0374200), *OsCKX10* (Os06g0572300), *OsCKX11* (Os08g0460600), *OsMADS25* (Os04g0304400), *OsMADS57* (Os02g0731200), *OsTB1* (Os03g0706500), *OsT20* (Os12g0405200), *OsD27* (Os11g0587000), *OsD17* (Os04g0550600), *OsD10* (Os01g0746400), *OsD3* (Os06g0154200), *OsD14* (Os03g0203200), *OsPIN2* (Os06g0660200), *OsWOX11* (Os07g0684900), *OsRR1* (Os04g0442300), *OsRR2* (Os02g0557800), *OsRR3* (Os02g0830200), *OsRR4* (Os01g0952500), *OsRR5* (Os04g0524300), *OsRR6* (Os04g0673300), *OsRR7* (Os07g0449700), *OsRR9* (Os11g0143300), *OsRR10* (Os12g0139400), and *OsRR11* (Os02g0631700).

RESULTS

OsCKX family genes display different expression patterns

Similar to the findings of previous studies, the *OsCKX* phylogenetic tree consisted of five major clades (Figure 1A). *OsCKX1*, which is commonly expressed in the roots, flowers, and grains, and *OsCKX2* were grouped together in the first clade. The β-glucuronidase (GUS) staining results revealed that *OsCKX1* had high expression in the shoot base and top of axillary buds, but very low expression in the leaf blade (Figure 1B). On the other hand, *OsCKX2*, usually expressed at high levels in the leaf sheath and inflorescence, was found to be highly expressed in the lateral root primordium, leaf blade, shoot base, and inflorescence. *OsCKX6*, *OsCKX7*, and *OsCKX10* were grouped together in the second clade and showed very low expression in all the tissues analyzed.

The third clade was composed of *OsCKX4*, *OsCKX5*, and *OsCKX9*. *OsCKX4*, which is generally strongly expressed in the vegetative organs, displayed extremely high expression in the roots. *OsCKX9* was generally expressed at low levels in all the tissues analyzed but showed special expression in the leaf blade and whole axillary buds. *OsCKX5*, usually highly expressed in all the checked tissues, also exhibited high expression in the roots and leaves.

The fourth clade consisted of *OsCKX3* and *OsCKX8*. *OsCKX3*, which is expected to have the highest expression in the stem and young panicles, was found to have high expression in the shoot base and young panicle. *OsCKX8*, commonly expressed at lower levels than *OsCKX3* in all vegetative organs, was highly expressed in the shoot base, flag leaf primordia, and inflorescence.

OsCKX11 showed a different sequence from other *OsCKX* genes; it was generally expressed at a higher level in all tissues, specifically in the reproductive-stage root and inflorescence, displaying high expression in the root, shoot base, and young inflorescence.

Cytokinins have many functions during plant growth and development in different organs, and the biodegradation of cytokinins in different periods or tissues can help plants accurately regulate their growth and development, so that each *OsCKX* gene is expressed in a distinct pattern. In rice, we found all of eight of the *OsCKX* genes expressed at the shoot base and inflorescence meristem at different stages and positions. We found some tissues with low expression of certain *OsCKX* genes, such as *OsCKX1* and *OsCKX3*, which were expressed at very low levels in the leaves, and *OsCKX2*, *OsCKX3*, and *OsCKX11*, which were expressed at very low levels in the flag leaf primordia. Additionally, we determined the expression patterns of *OsCKX* genes in axillary buds: *OsCKX1* was expressed at the top; *OsCKX2*, *OsCKX3*, *OsCKX4*, and *OsCKX5* were expressed at the base; and *OsCKX9* was expressed throughout the buds.

***OsCKX* mutants exhibit different phenotypes**

Previous studies suggested that the knockdown of specific *OsCKXs* might help improve rice production by influencing important agronomic traits, such as tillering, development of organs facilitating nutrition, and panicle phenotype. To confirm this hypothesis, we created mutants of all OsCKX genes using CRISPR/Cas9 system, including single mutants of nine OsCKXs (except *OSCKX6* and *OSCKX10*), double mutants of *OSCKX1/2* and *OSCKX4/9*, and triple mutants of *OSCKX6/7/10* (Supplemental Figures S1-S3).

Since leaf size affects the photosynthetic capacity of rice, we investigated this and discovered that the top three leaves in the *osckx1*, *osckx2*, *osckx8*, and *osckx11* mutants were distinctly longer and wider compared to those of Zhonghua 11 (Supplemental Figures S4-S6; Supplemental Table S2). The last three leaves of the *osckx9* mutant were also distinctly longer, yet no change in their width was observed compared to Zhonghua 11. The leaf length and width of the other mutants did not

significantly change (Supplemental Figures S5, A–D, and S6). On the other hand, culm diameter and plant height are closely related to the lodging resistance of rice. We found that the diameters of the basal internodes in *osckx1*, *osckx2*, *osckx8*, and *osckx11* mutants were significantly wider than those in the WT, while the *osckx3*, *osckx4*, and *osckx5* mutants had thinner basal internodes (Supplemental Figure S5, E and F). Furthermore, the *osckx3*, *osckx4*, and *osckx5* mutants showed significantly decreased plant height compared to others (Supplemental Figure S5, G and H).

The panicle number is determined by the tiller number per plant and has a significant effect on rice yield. In the field and pot experiments, the *osckx4* and *osckx9* mutants developed more tillers than the WT plants, which is consistent with the results of previous studies (Supplemental Figures S4B and S5, I and J; Supplemental Tables S2 and S3). Although the mutants produced more panicles per plant, the number of grains per panicle decreased, resulting in no significant change in yield (Supplemental Figure S7, A-D; Supplemental Table S2). In contrast, the *osckx2* mutant showed significantly reduced tiller number in both the 2019 and 2020 field and pot experiments (Supplemental Tables S2 and S3). However, no significant differences were observed in the tiller numbers of the other *osckx* mutants. Additionally, there was no significant change in the yield per plant of the *osckx* mutants, except for *osckx1* and *osckx11-1*, which had significantly improved production. In contrast, *osckx3-1*, *osckx3-26*, and *osckx4-6* had significantly low yields (Supplemental Figures S7, A and B). Despite this, we observed several agronomic traits that were improved in the mutants. For example, the *osckx1*, *osckx2*, *osckx7*, and *osckx8* mutants presented heavier grain weight, while the *osckx11* mutant developed more spikelets per panicle (Supplemental Figure S7, E–H).

As OsCKX6, OsCKX7, and OsCKX10 have a similar protein sequence, the corresponding genes have very low expression levels. Using these genes, we constructed *osckx6/7/10* triple mutant lines; all

the three lines showed no significant difference in panicle number and yield compared to the WT (Supplemental Figures S8).

The *osckx1 osckx2* double mutants have significantly reduced tiller numbers

In 2021, both of the two *osckx1/2* lines showed a significant increase in the number of spikelets per panicle in relation to NIP+; this increase is mainly attributed to the significantly increased number of primary branches per panicle; however, the *osckx1/2-19* mutant showed a significant increase in the number of secondary branches per panicle (Figure 2, A–D). A similar phenotype was also seen in 2020 (Supplemental Figure S9, A–D). However, compared to NIP, the seed setting rate of *osckx1/2* mutant lines was significantly lower in the two years (Figure 2E, Supplemental Figure S9E). Furthermore, the panicle number of *osckx1/2* mutant lines was less than that of NIP in 2021, while the *osckx1/2-19* mutant showed a significantly reduced number of tillers and panicles per plant compared to NIP in 2020 (Figure 2F, Supplemental Figure S9, F and G). Moreover, the 1,000-grain weight and grain length were significantly increased in *osckx1/2-19* compared with those in NIP (Supplemental Figure S9, H–J). In contrast, the grain width and thickness did not show significant changes between *osckx1/2-19* and NIP (Supplemental Figure S9, K and L). Owing to the small panicle number per plant and lower setting rate, the yield of *osckx1/2* lines was lower compared to that of NIP (Figure 2G, Supplemental Figure S9M). Moreover, in *osckx1/2-19* plants, the flag leaf became wider (Supplemental Figure S9, N and O) and the plants had thick basal internodes, while the plant height did not noticeably change (Supplemental Figure S9, P and Q). Collectively, these observations of the spikelet phenotype, panicle number, and vegetative organ size suggest that the double knockout of *OsCKX1* and *OsCKX2* may help improve the lodging resistance and optimize the plant architecture in rice.

Double knockout of *OsCKX4* and *OsCKX9* significantly promotes tillering

As expected, we discovered that the *osckx4/9* double mutant had an extremely higher tiller number compared to NIP and the two single mutants (Figure 3, A–D). In contrast, panicle size was significantly reduced in the *osckx4/9* mutant (Figure 3E). The *osckx9-1* mutant had a high panicle number per plant, but the number was markedly higher in the *osckx4/9* mutant (Figure 3F). However, the number of spikelets per panicle of *osckx4* was significantly decreased, while that of *osckx4/9* was even lower (Figure 3G). The decreased number of spikelets per panicle of *osckx4-6* was due to the low number of secondary branches per panicle, while the low number of spikelets per panicle of *osckx4/9* was caused by the reduced number of both the primary and secondary branches (Figure 3, E, H, and I). On the other hand, seed setting rates were similar in the single and double mutants, and were significantly lower than those in WT (Figure 3J). Despite the increase in grain length, the *osckx4-6* mutant presented decreased 1,000-grain weight due to reduced grain thickness (Figure 3K; Supplemental Figure S10, A–E). The 1,000-grain weight of *osckx4/9* was lower than that of the *osckx4-6* mutant due to reduced grain width and thickness (Figure 3K; Supplemental Figure S10, A-E). As a result of these changes, the yield of *osckx4/9* was significantly decreased (Figure 3L). Moreover, the root length, diameter of basal internode, plant height, and flag leaf length and width were further decreased in the double mutant compared to those in the two single mutants (Figure 3, A, M and N; Supplemental Figure S10, F-H).

We also conducted a hydroponic experiment to investigate the root phenotypes of the mutants (Figure 4A). We verified that *OsCKX4* and *OsCKX9* have redundant roles in regulating tillering, plant height, and root length (Figure 4 B and C). The *osckx4/9* mutant not only had shorter roots, but also fewer crown roots and smaller root diameter (Supplemental Figure S11, A and B). The length and width of the 8th leaf were also decreased in *osckx4-6* and *osckx4/9* compared to those in NIP (Figure 4, D and E). These results indicate that the reduction in the leaf size of *osckx4/9* started at the vegetative stage.

Overall, these results suggest that *OsCKX4* and *OsCKX9* have a functional overlap during rice growth and development.

RNA-seq analysis reveals the molecular functions of *OsCKX4* and *OsCKX9*

To obtain information regarding the possible functional context of *OsCKX4* and *OsCKX9*, we sampled the roots and shoot bases from NIP, *osckx4*, *osckx9*, and *osckx4/9* and performed RNA-seq analysis. Results revealed that *osckx4* had 297 differentially expressed genes (DEGs) in the shoot bases and 415 DEGs in the roots. There were 500 DEGs in the shoot bases and 342 DEGs in the roots of the *osckx9* mutant. The *osckx4/9* double mutant had the highest number of DEGs, with 806 DEGs in the shoot base and 4,556 DEGs in the roots (Figure 5A). To verify the accuracy and reproducibility of the RNA-seq results, we randomly selected seven previously studied genes associated with the phenotypes observed in this study for quantitative reverse-transcription PCR analysis. The expression profiles of these genes were found to corroborate the RNA-seq results (Supplemental Figure S12).

However, although there were numerous DEGs between the WT and mutants, there were 71 DEGs in the roots and 90 DEGs in the shoot bases that overlapped between the *osckx4* vs. WT and *osckx9* vs. WT comparisons and occupied only a small fraction of the total DEGs (Figure 5B). These included some genes that regulate the absorption of silicon (*Lsi1*, *Lsi2*), zinc (*OsZIP16*), and iron (*OsIRO2*) (Fig 5C). *OsZIP9*, *OsTCP19*, *OsHKT1.1*, and *OsNPF5.5* were upregulated in the shoots of *osckx4*, while *OsLBD37*, *OsARF19*, *OsMYB61*, and *MT1a* were upregulated in the shoots of *osckx9*. In the roots, the downregulation of *OsAAP5*, *OsAAP8*, and *OsNLP6* and the upregulation of certain genes influenced the iron and phosphorus absorption in *osckx4*. We also observed the downregulation of *OsPUP1*, *OsPUP5*, *OsRR10*, and *OsNAAT4* in *osckx9*. These DEGs were also revealed to be associated with the different pathways controlled by *OsCKX4* and *OsCKX9* (Figure 5C). However, the functions of most

DEGs remain unknown (Supplemental Dataset 1). The difference in the number of DEGs identified may imply that *OsCKX4* and *OsCKX9* have different functions. Moreover, 87.1% and 78.2% of DEGs in the roots and shoot bases, respectively, between the *osckx4/9* and WT were identified only in the double mutants, which may have been caused by the duplicate effect of the functional loss of *OsCKX4* and *OsCKX9* (Figure 5B).

Since we observed that *osckx4/9* exhibited more severe phenotypes and possessed more DEGs, we analyzed the DEGs identified in the roots and shoot bases between the WT and *osckx4/9* plants by using Kyoto Encyclopedia of Genes and Genomes (KEGG) enrichment analysis (Figure 5D). In both tissues, the top enriched KEGG pathways included 'glycolysis/gluconeogenesis', 'biosynthesis of amino acids', and those related to carbon and nitrogen metabolism. Since most of the DEGs were not functionally annotated, the relationship between the DEGs and the enriched pathways and their influence on the growth and development of the mutant plants were not fully understood. However, we identified several genes that may be associated with the phenotypes observed in this study.

OsCKX4 and OsCKX9 regulate cytokinin levels

As OsCKX4 and OsCKX9 are involved in biodegradation of cytokinins, we first analyzed the DEGs associated with cytokinin metabolism and signal transduction. Among the cytokinin metabolism-related genes, only *OsCKX2* and *OsCKX5* expression was downregulated in the root of *osckx4/9* (Supplemental Dataset 1).

Type-A *OsRR* genes are a group of genes that can be induced by cytokinins. However, the expression of *OsRR4*, *OsRR6*, *OsRR7*, *OsRR9*, and *OsRR10* was significantly downregulated in the roots of *osckx4/9*, whereas the expression of *OsRR10* was significantly downregulated in the roots of *osckx9* (Figure 6A). In the shoot base, only *OsRR10* expression was significantly upregulated in *osckx9* and

osckx4/9 mutants (Figure 6A). In contrast, in the axillary bud, the expression of detectable type-A *OsRR* genes, except *OsRR2*, was significantly upregulated in *osckx4/9* mutants (Figure 6B).

Although type-A *OsRR* genes can indicate the content of cytokinins indirectly, we sampled the roots and shoot base of NIP and *osckx4/9* to detect the content of cytokinins. In the root, compared to NIP, the content of cZ, iP, tZ, IPA, and tZR showed a significant increase, while 6-BA and DHZR contents significantly decreased in *osckx4/9* (Figure 6C). However, in the shoot base, we found a higher content of iP and lower content of tZR and DHZR in *osckx4/9* (Figure 6D).

SL metabolism and signaling are not regulated by *OsCKX4* and *OsCKX9*

SLs perform the function of regulating tiller numbers. To investigate the cause of the increased tiller numbers in the single and double mutants, we examined the genes associated with SLs. In the root and shoot base, none of the genes related to SL biosynthesis and signaling transduction, including *OsT20* (Liu *et al*., 2020), *OsD27*, *OsD17*, *OsD10*, *OsD3*, *OsD14*, and *OsD53*, showed significant difference between NIP and mutants (Figure 7A). In axillary buds, only the expression of *OsD17* in *osckx4/9* was significantly downregulated (Figure 7B). Moreover, expression of the SL signaling-related transcription factor *OsTB1* showed no significant change in the root and shoot base between NIP and mutants but was significantly upregulated in the axillary buds of the *osckx4/9* mutant compared to NIP (Figure 7, A and B), whereas *OsMADS57* expression was significantly downregulated in the roots of *osckx4/9* mutants (Figure 7A). Based on these results, there is no direct evidence that the metabolism and signaling transduction of SLs are downstream of *OsCKX4* and *OsCKX9*.

***OsCKX4* and *OsCKX9* may participate in regulating the metabolism and transport of other hormones**

First, we identified genes related to gibberellin metabolism. We found that the expression of *OsKS1* and

OsKS2 was significantly downregulated in the roots of *osckx4/9* (Figure 8; Supplemental Dataset 1). OsKS1 and OsKS2 are enzymes involved in gibberellin biosynthesis. The expression of *OsKS2* was downregulated in the roots of the *osckx9* mutant, while no changes were observed in the *osckx4* mutant. Other genes for GA biosynthesis and degradation, such as *GA20ox* and *GA2ox*, were markedly downregulated in the roots of the *osckx4/9* mutant. Some GA receptors were also downregulated in the roots of the *osckx4/9* mutant. The changes in the expression of gibberellin-related genes may explain the significantly reduced plant height of *osckx4/9* double mutants.

Additionally, investigation of several differentially expressed auxin-related genes revealed that auxin efflux transporters *OsPIN2* and *OsPIN8* were upregulated in the shoot bases and the roots, respectively, of the mutants. We found that the auxin primary response genes *OsGH3-1*, *OsGH3-2*, *OsIAA9*, and *OsSAUR12* were upregulated in the shoot bases of the *osckx4/9* and single mutants. Additionally, *OsGH3-2*, nine *OsIAA* genes (*OsIAA1, 4, 9, 12, 14, 15, 19, 23, 24*), and five *OsSAUR* genes (*OsSAUR6, 20, 27, 28, 33*) were downregulated in the roots of *osckx4/9*; however, *OsIAA16* was upregulated in the roots of *osckx4/9*.

DISCUSSION

Functional differences and redundancy between *OsCKX* genes

To systematically determine the functions of *OsCKX* genes, we analyzed their expression patterns and investigated the phenotypes of *osckx* single, double and triple mutation lines. Our study revealed the roles of all *OsCKX* genes in the growth and development of rice. After two years of field experiments, we discovered that *osckx4* and *osckx9* developed more tillers at the vegetative stage, while *osckx2* had fewer tillers. At the reproductive stage, the top three leaves were longer and wider and the basal internodes were thicker in *osckx1*, *osckx2*, *osckx8*, and *osckx11* (Zhonghua11 [ZH11] background), while wider flag leaves and thicker basal internodes were observed in *osckx1/2* (NIP background) (Figure 9). The *osckx9*, *osckx3*, *osckx4*, and *osckx5* mutants showed little changes in flag leaf length and width compared to their background, while *osckx3*, *osckx4*, and *osckx5* developed thinner basal internodes. For yield-related phenotypes, *osckx9* developed more panicles while *osckx9* and *osckx4* had fewer spikelets per panicle. Moreover, *osckx1*, *osckx2*, and *osckx8* displayed increased 1,000-grain weight, while *osckx11* showed reduced 1,000-grain weight.

Previous studies have described the functions of *OsCKX2*, *OsCKX4*, *OsCKX9*, and *OsCKX11*. First, researchers elucidated the function of *OsCKX2* after observing that null mutants or plants with downregulation of *OsCKX2* developed more spikelets per panicle (Ashikari *et al.*, 2005), more tillers, and larger grains (Yeh *et al.*, 2015). In the present study, we observed very little increase in the number of spikelets per panicle during the two-year field experiment, with the observed increase being lower than that observed by the other researchers. However, we found that the *osckx2* mutant of ZH11 showed significantly reduced tiller number within the first year of the field experiment. Another mutant, *osckx1/2* of NIP, also showed a reduced tiller number, which supports the hypothesis that fewer tillers

may be related to thicker culms. Furthermore, both the *osckx2* mutant of ZH and *osckx1/2* mutant of NIP presented increased 1,000-grain weight. The discrepancies between our results and previous findings regarding panicle size may be attributed to the different cultivated varieties or environmental impact.

Furthermore, previous reports stated that *OsCKX4* overexpression can cause the development of a larger root system, but result in shorter plant height, fewer tillers, and smaller panicles (Gao *et al.*, 2014). Moreover, *OsCKX4-RNAi* or *osckx4* mutants showed fewer crown roots and shorter root lengths (Gao *et al.*, 2014; Mao *et al.*, 2020). Since *OsCKX4* is commonly expressed in the root, previous studies were more focused on investigating the relationships between *OsCKX4* and the root system instead of the shoot system. Here, we discovered that *osckx4* mutants produced more tillers, especially at the early stages, but has fewer spikelets per panicle. Additionally, *osckx9* mutants have been reported to develop more tillers, fewer spikelets per panicle, and shorter plant height (Duan *et al.*, 2019). Since the null mutations of *OsCKX4* and *OsCKX9* can affect the tiller number, we constructed *osckx4/9* mutants, which distinctly showed more tillers, shorter plant height, and smaller panicles. The increase in the tiller number of *osckx4/9* double mutants was greater than observed in *osckx4* and *osckx9* single mutants. Furthermore, the decrease in plant height and number of spikelets per panicle of *osckx4/9* double mutants was also higher than observed in *osckx4* and *osckx9* single mutants. These results suggest the partial functional overlap of *OsCKX4* and *OsCKX9* during rice growth and development. Moreover, *osckx11* mutants previously displayed more tillers, larger panicles, and lighter 1,000-grain weight (Zhang *et al.*, 2020); these were also observed in our study.

Exceeding our expectations, none of the single mutants showed a stable significant increase in yield, while the double mutants *osckx1/2* and *osckx4/9* showed lower yields. These results may be

attributed to the check and balance of yield factors. For instance, *osckx1/2* had a larger panicle and higher 1000-grain weight as well as a reduced panicle number and lower seed setting rate. *osckx4/9* also had larger amount of panicle number but smaller panicles, lighter 1000-grain weight and lower seed setting rate. With knowledge of the phenotypes of these mutants, to improve the yields, future studies should develop mutants exhibiting advantageous characteristics and lacking the undesirable attributes.

In general, we found that each *OsCKX* gene had its own function during rice growth and development as well as their own distinct characteristics, and each *osckx* single or double mutant had a distinct phenotype, but why these different phenotypes happen need to be explored in depth.

Potential causes of the functional differences and redundancy in *OsCKX* genes

The main function of CKX enzymes is the biodegradation of cytokinins. Previous studies have reported that CKXs catalyze different kinds of cytokinins. In maize, the ZmCKX enzyme activity has been systematically analyzed; for example, ZmCKX1 and ZmCKX12 specifically target iP, tZ, and cZ (Zalabak *et al.*, 2014). In *Arabidopsis*, AtCKX1 showed the highest preference for tZ phosphates, iP phosphates, and iP9G, while AtCKX3 preferred iP phosphates and iPR, and AtCKX7 preferred iP9G and tZ (Kowalska *et al.*, 2010). However, little is known about the preference of OsCKX enzymes, in vitro experiment shows OsCKX9 that is partial to tZ and OsCKX11 that specially targets tZ and cZ (Duan *et al.*, 2019; Zhang *et al.*, 2020). OsCKX11 has the same substrate as its homolog protein, ZmCKX10, while other OsCKX enzyme substrates may need to be inferred from endogenous hormone content data. From the hormone content detected in the root of *OsCKX4-overexpression* line, it was found that the content of iP and tZ cytokinin showed no obvious change compared to WT, while DHZ and the combined type of iP and tZ showed a significant reduction (Gao *et al.*, 2014). In our study, in

the root and shoot base, not all kinds of cytokinins showed higher levels in *osckx4/9* mutants. Therefore, the distinctive functions of OsCKXs may be attributed to their different target substrates.

CKX proteins are mainly localized in the ER because most contain an N-terminal signal peptide sequence (Niemann *et al.*, 2018; Zalabak *et al.*, 2016). In the ER, cytokinins combine with their receptors and initiate signaling transduction, while most ER-localized CKXs regulate cytokinin concentrations to precisely adjust cytokinin signals (Niemann *et al.*, 2018; Romanov and Schmulling, 2021). Previous studies revealed that OsCKX4 and OsCKX11 are localized in the cytosol, while OsCKX9 is localized in the cytosol and nuclei (Duan *et al.*, 2019; Gao *et al.*, 2014; Zhang *et al.*, 2020). These three CKXs potentially regulate the cytokinin balance in other cellular organelles. However, the locations of the remaining OsCKXs remain unknown. Hence, we hypothesize that the subcellular localization of OsCKXs may also influence their functional differentiation.

In this study, the *OsCKX* genes exhibited different expression patterns. For example, *OsCKX1* and *OsCKX2* were expressed in the flower and grains, but *OsCKX1* showed lower expressed in the inflorescence meristem, which is the same as the previous study (Ashikari *et al.*, 2005). As *OsCKX4* and *OsCKX9* showed similar phenotypes in tiller number, the expression pattern showed a considerable difference. *OsCKX4* has a high expression highly in nutrition organs, yet the expression of *OsCKX9* in these organs is very low, and the different expression can get illation from previous studies (Duan *et al.*, 2019; Gao *et al.*, 2014). In inflorescence meristem, the two genes showed low expression level, which is also the same as previous studies by RT-southern blot (Ashikari *et al.*, 2005). In summary, the differences in the nature of catalytic substrates, subcellular localization, and expression in tissues may contribute to the different functions observed in *OsCKX* family genes.

Significantly altered transcriptome of the *osckx4 osckx9* mutant

Although *OsCKX4* and *OsCKX9* have been extensively studied, we observed new phenotypes in the single mutants, which have not been reported previously. Interestingly, these two genes were found to exhibit redundant functions during rice growth and development. Hence, we first investigated the genes associated with plant height and then identified the DEGs related to gibberellin metabolism between the NIP and mutants. *OsKS1* and *OsKS2*, which encode enzymes that catalyze the second step of the GA biosynthesis pathway (Ji *et al.*, 2014; Tezuka *et al.*, 2015), were significantly downregulated in the roots of *osckx4/9*. On the other hand, possibly due to the limited substrate, the expression of several *GA20ox* and *GA2ox* genes for gibberellin biosynthesis and biodegradation, respectively, were downregulated in *osckx4/9*. We hypothesize that the disrupted biosynthesis of gibberellin may have caused the reduction in *osckx4/9* plant height. However, the mechanism by which *OsCKX4* and *OsCKX9* regulate the expression of *OsKS1* and *OsKS2* is unknown.

Since the double mutants exhibited semi-dwarf phenotypes with more tillers, we suspected that the expression of SL-related genes may have changed in the double mutants. However, we did not observe any changes in the expression of SL biosynthesis- and signaling-related genes in the shoot base or the root but found that *OsD17* expression was downregulated in the axillary bud of *osckx4/9* mutants. However, expression of the SL-related transcription factor *OsTB1* was upregulated in the axillary bud, whereas *OsMADS57* expression was only downregulated in the roots. Previous studies on *tb1* mutants and *OsMADS57* overexpression showed that these plants developed more tillers than the WT (Guo *et al.*, 2013; Takeda *et al.*, 2003). Since SL directly activates *OsCKX9* to regulate shoot architecture in rice, we also determined whether *OsCKX4* and *OsCKX9* can regulate the tiller number phenotype through the SL pathway by analyzing the expression of SL-related genes between WT and mutants. Based on these findings, cytokinin may be located downstream of the SL pathway during rice tillering.

During the outgrowth of tiller buds, the auxin at the tip of the axillary bud is transported by auxin efflux carriers. In *Arabidopsis*, cytokinin response factors regulate *PIN* expression (Simaskova *et al.*, 2015; Waldie and Leyser, 2018). Here, we found that *OsPIN2* was upregulated in the shoot bases of *osckx4* and *osckx4/9*. In rice, OsPIN2 transports auxins from the shoot to the root–shoot junction, and overexpression of *OsPIN2* results in the increased number of tillers (Chen *et al.*, 2012). Moreover, in *OsCKX4-overexpression* line, the content of IAA is significantly reduced in root and the expression of *OsPIN1b* and *OsPIN2* showed significantly lower (Gao *et al.*, 2014), the connection between cytokinin and auxin transporters is needed for further research.

In addition, we found that several type-A transcription factors, including *OsRR4*, *OsRR6*, *OsRR7*, *OsRR9*, and *OsRR10*, showed lower expression in the roots of *osckx4/9*, and *OsRR10* expression was downregulated in the roots of *osckx9* mutants. However, considering the higher content of most kinds of cytokinins in the root of *osckx4/9* mutants, these results were contradictory, since type-A RR genes are primary response genes for cytokinin signaling. Lower expression of some type-A *OsRR* genes may be caused by the local deficiency of cytokinins in the root tips of *osckx4/9*, and the higher cytokinin level of roots in *osckx4/9* seemed to relate to the loss of function of OsCKX4 and OsCKX9 in the vascular tissue of the root. The expression of type-A *OsRR* genes, except *OsRR10*, did not significantly change, but the levels of some kinds of cytokinins changed; this finding suggests the functional variety of cytokinins. Finally, the upregulation of expression of nine type-A *OsRR* genes in the axillary buds of *osckx4/9* may have resulted from the increase in the level of cytokinins; however, owing to the limitations of the technique used, the content of cytokinins in this tissue remains unknown. In the present study, we observed the downregulation of *OsMADS25* (Yu *et al.*, 2015) in the roots of *osckx4/9*, which may explain why *osckx4* and *osckx4/9* plants have smaller root systems. However, the

mechanisms underlying this process are unknown; hence, further research is still required.

Interestingly, in addition to the genes regulated by both *OsCKX4* and *OsCKX9*, we also identified several genes that are regulated by *OsCKX4* and *OsCKX9* individually. In summary, the similar amino acid sequences but different expression patterns and different subcellular localization of *OsCKX4* and *OsCKX9* enable them to functionally overlap in the regulation of some pathways, while also individually regulating specific pathways.

In conclusion, our systematic analysis of 11 genes in the OsCKX family reveals their complex expression patterns in rice. A total of 27 *OsCKX* mutantation lines were produced using CRISPR/Cas9 technology. By examining the phenotypes of the mutants throughout the rice growth period, we determined the functions of specific *OsCKX* genes in plant development. In specific, we discovered that *OsCKX4* and *OsCKX9* inhibited tillering, while *OsCKX1* and *OsCKX2* promoted tillering. Considered together, our findings establish a community resource for fully elucidating the function of *OsCKXs*, providing new insights that may be used for future studies to improve rice yield and initiate green production.

Supplemental data

The following supplemental materials are available.

Supplemental Figure S1. Gene structures and mutation details of *OsCKXs*.

Supplemental Figure S2. Chromatograms of the *osckx* mutant lines.

Supplemental Figure S3. Mutation details and chromatograms of double and triple mutants

Supplemental Figure S4. The *osckx* mutants of Zhonghua11 from the 2020 field experiment.

Supplemental Figure S5. Phenotypic characterization of the vegetative organs in *osckx* mutants from the 2020 field experiment.

Supplemental Figure S6. Phenotypic characterization of the second and third top leaves in *osckx* mutants from the 2020 field experiment.

Supplemental Figure S7. Phenotypic characterization of yield-related phenotypes in *osckx* mutants from the 2020 field experiment.

Supplemental Figure S8. Phenotypic characterization of the yield and panicles per plant in Nipponbare (NIP) and *osckx6/7/10* plants.

Supplemental Figure S9. Phenotypic characterization between Nipponbare (NIP) and *osckx1/2-19* mutant plants in 2020.

Supplemental Figure S10. Phenotypic characterization of the flag leaves and seeds in Nipponbare (NIP), *osckx4*, *osckx9*, and *osckx4/9* plants.

Supplemental Figure S11. Phenotypic characterization of the leaf and root systems in wild-type and *osckx4/9* plants.

Supplemental Figure S12. Relative expression levels and FPKM values of *D17*, *RR4*, *WOX11*, *PIN2*, *TB1*, *OsMADS25*, and *OsMADS57* in the roots and shoot bases (BP) of Nipponbare (NIP), *osckx4*,

osckx9, and *osckx4/9*.

Supplemental Table S1. Information of primers used in the study.

Supplemental Table S2. Characterization of the vegetative organs and yield-related phenotypes in *osckx* mutants from the 2019 field experiment.

Supplemental Table S3. Tiller numbers in *osckx* mutants from the 2019 field experiment.

Supplemental Dataset 1. RNA sequencing data.

Funding:

This work was supported by the National Natural Science Foundation of China (Grant number 31872855 and 31971842).

Data availability

All data supporting the findings of this study are available within the paper and within its supplementary data published online.

Acknowledgments

We thank Jiankang Zhu and Caixia Gao for providing the vectors of the CRISPR-Cas9 system. We also thank Biogle and Biorun genome editing center for producing transgenic rice.

Author contributions

C.D. and Y.D. conceived the original screening and research plans; C.R., Y.L., Z.C., Z.L., and C.D. performed the experiments and analyzed the data; C.R. and C.D. wrote the article with contributions of all the authors; C.D. agrees to serve as the author responsible for contact and ensures communication.

Conflict of interest

The authors declare no competing interests in relation to this work.

Reference

Ashikari M, Sakakibara H, Lin S, Yamamoto T, Takashi T, Nishimura A, Angeles ER, Qian Q, Kitano H, Matsuoka M. 2005. Cytokinin oxidase regulates rice grain production. Science **309**, 741-745.

Bartrina I, Otto E, Strnad M, Werner T, Schmulling T. 2011. Cytokinin regulates the activity of reproductive meristems, flower organ size, ovule formation, and thus seed yield in Arabidopsis thaliana. Plant Cell **23**, 69-80.

Cai BD, Zhu JX, Shi ZG, Yuan BF, Feng YQ. 2013. A simple sample preparation approach based on hydrophilic solid-phase extraction coupled with liquid chromatography-tandem mass spectrometry for determination of endogenous cytokinins. J Chromatogr B **942-943**, 31-36.

Chen L, Zhao J, Song J, Jameson PE. 2020. Cytokinin dehydrogenase: a genetic target for yield improvement in wheat. Plant Biotechnol J **18**, 614-630.

Chen Y, Fan X, Song W, Zhang Y, Xu G. 2012. Over-expression of OsPIN2 leads to increased tiller numbers, angle and shorter plant height through suppression of OsLAZY1. Plant Biotechnol J **10**, 139-149.

Duan J, Yu H, Yuan K, Liao Z, Meng X, Jing Y, Liu G, Chu J, Li J. 2019. Strigolactone promotes cytokinin degradation through transcriptional activation of CYTOKININ OXIDASE/DEHYDROGENASE 9 in rice. Proc Natl Acad Sci U S A **116**, 14319-14324.

Gao S, Fang J, Xu F, Wang W, Sun X, Chu J, Cai B, Feng Y, Chu C. 2014. CYTOKININ OXIDASE/DEHYDROGENASE4 Integrates Cytokinin and Auxin Signaling to Control Rice Crown Root Formation. Plant Physiol **165**, 1035-1046.

Guo S, Xu Y, Liu H, Mao Z, Zhang C, Ma Y, Zhang Q, Meng Z, Chong K. 2013. The interaction between OsMADS57 and OsTB1 modulates rice tillering via DWARF14. Nat Commun **4**, 1566.

Jameson PE, Song J. 2020. Will cytokinins underpin the second 'Green Revolution'? J Exp Bot **71**, 6872-6875.

Ji SH, Gururani MA, Lee JW, Ahn BO, Chun SC. 2014. Isolation and characterisation of a dwarf rice mutant

exhibiting defective gibberellins biosynthesis. Plant Biol (Stuttg) **16**, 428-439.

Kanehisa M. 2019. Toward understanding the origin and evolution of cellular organisms. Protein Science **28**, 1947-1951.

Kollmer I, Novak O, Strnad M, Schmulling T, Werner T. 2014. Overexpression of the cytosolic cytokinin oxidase/dehydrogenase (CKX7) from Arabidopsis causes specific changes in root growth and xylem differentiation. Plant J **78**, 359-371.

Kowalska M, Galuszka P, Frebortova J, Sebela M, Beres T, Hluska T, Smehilova M, Bilyeu KD, Frebort I. 2010. Vacuolar and cytosolic cytokinin dehydrogenases of Arabidopsis thaliana: heterologous expression, purification and properties. Phytochemistry **71**, 1970-1978.

Kumar S, Stecher G, Li M, Knyaz C, Tamura K. 2018. MEGA X: Molecular Evolutionary Genetics Analysis across Computing Platforms. Mol Biol Evol **35**, 1547-1549.

Kurakawa T, Ueda N, Maekawa M, Kobayashi K, Kojima M, Nagato Y, Sakakibara H, Kyozuka J. 2007. Direct control of shoot meristem activity by a cytokinin-activating enzyme. Nature **445**, 652-655.

Li S, Zhao B, Yuan D, Duan M, Qian Q, Tang L, Wang B, Liu X, Zhang J, Wang J, Sun J, Liu Z, Feng YQ, Yuan L, Li C. 2013. Rice zinc finger protein DST enhances grain production through controlling Gn1a/OsCKX2 expression. Proc Natl Acad Sci U S A **110**, 3167-3172.

Liu X, Hu Q, Yan J, Sun K, Liang Y, Jia M, Meng X, Fang S, Wang Y, Jing Y, Liu G, Wu D, Chu C, Smith SM, Chu J, Wang Y, Li J, Wang B. 2020. zeta-Carotene Isomerase Suppresses Tillering in Rice through the Coordinated Biosynthesis of Strigolactone and Abscisic Acid. Mol Plant 13, 1784-1801.

Madeira F, Park YM, Lee J, Buso N, Gur T, Madhusoodanan N, Basutkar P, Tivey ARN, Potter SC, Finn RD, Lopez R. 2019. The EMBL-EBI search and sequence analysis tools APIs in 2019. Nucleic Acids Res **47**, W636-W641.

Mao C, He J, Liu L, Deng Q, Yao X, Liu C, Qiao Y, Li P, Ming F. 2020. OsNAC2 integrates auxin and cytokinin pathways to modulate rice root development. Plant Biotechnol J **18**, 429-442.

Mao Y, Zhang H, Xu N, Zhang B, Gou F, Zhu JK. 2013. Application of the CRISPR-Cas system for efficient genome engineering in plants. Mol Plant **6**, 2008-2011.

Niemann MCE, Weber H, Hluska T, Leonte G, Anderson SM, Novak O, Senes A, Werner T. 2018. The Cytokinin Oxidase/Dehydrogenase CKX1 Is a Membrane-Bound Protein Requiring Homooligomerization in the Endoplasmic Reticulum for Its Cellular Activity. Plant Physiol **176**, 2024-2039.

Osugi A, Kojima M, Takebayashi Y, Ueda N, Kiba T, Sakakibara H. 2017. Systemic transport of trans-zeatin and its precursor have differing roles in Arabidopsis shoots. Nat Plants **3**, 17112.

Romanov GA, Schmulling T. 2021. Opening Doors for Cytokinin Trafficking at the ER Membrane. Trends Plant Sci **26**, 305-308.

Schwarz I, Scheirlinck MT, Otto E, Bartrina I, Schmidt RC, Schmulling T. 2020. Cytokinin regulates the activity of the inflorescence meristem and components of seed yield in oilseed rape. J Exp Bot **71**, 7146-7159.

Simaskova M, O'Brien JA, Khan M, Van Noorden G, Otvos K, Vieten A, De Clercq I, Van Haperen JMA, Cuesta C, Hoyerova K, Vanneste S, Marhavy P, Wabnik K, Van Breusegem F, Nowack M, Murphy A, Friml J, Weijers D, Beeckman T, Benkova E. 2015. Cytokinin response factors regulate PIN-FORMED auxin transporters. Nat Commun **6**, 8717.

Takeda T, Suwa Y, Suzuki M, Kitano H, Ueguchi-Tanaka M, Ashikari M, Matsuoka M, Ueguchi C. 2003. The OsTB1 gene negatively regulates lateral branching in rice. Plant J **33**, 513-520.

Tezuka D, Ito A, Mitsuhashi W, Toyomasu T, Imai R. 2015. The rice ent-KAURENE SYNTHASE LIKE 2 encodes a functional ent-beyerene synthase. Biochem Biophys Res Commun **460**, 766-771.

Tsai YC, Weir NR, Hill K, Zhang W, Kim HJ, Shiu SH, Schaller GE, Kieber JJ. 2012. Characterization of

genes involved in cytokinin signaling and metabolism from rice. Plant Physiol **158**, 1666-1684.

Waldie T, Leyser O. 2018. Cytokinin Targets Auxin Transport to Promote Shoot Branching. Plant Physiol **177**, 803-818.

Wang J, Xu H, Li N, Fan F, Wang L, Zhu Y, Li S. 2015. Artificial Selection of Gn1a Plays an Important role in Improving Rice Yields Across Different Ecological Regions. Rice (N Y) **8**, 37.

Wang WC, Lin TC, Kieber J, Tsai YC. 2019. Response Regulators 9 and 10 Negatively Regulate Salinity Tolerance in Rice. Plant Cell Physiol **60**, 2549-2563.

Wang Y, Lu Y, Guo Z, Ding Y, Ding C. 2020. RICE CENTRORADIALIS 1, a TFL1-like Gene, Responses to Drought Stress and Regulates Rice Flowering Transition. Rice (N Y) **13**, 70.

Werner T, Motyka V, Strnad M, Schmulling T. 2001. Regulation of plant growth by cytokinin. Proc Natl Acad Sci U S A **98**, 10487-10492.

Yeh SY, Chen HW, Ng CY, Lin CY, Tseng TH, Li WH, Ku MS. 2015. Down-Regulation of Cytokinin Oxidase 2 Expression Increases Tiller Number and Improves Rice Yield. Rice (N Y) **8**, 36.

Yu C, Liu Y, Zhang A, Su S, Yan A, Huang L, Ali I, Liu Y, Forde BG, Gan Y. 2015. MADS-box transcription factor OsMADS25 regulates root development through affection of nitrate accumulation in rice. PLoS One **10**, e0135196.

Zalabak D, Galuszka P, Mrizova K, Podlesakova K, Gu R, Frebortova J. 2014. Biochemical characterization of the maize cytokinin dehydrogenase family and cytokinin profiling in developing maize plantlets in relation to the expression of cytokinin dehydrogenase genes. Plant Physiol Biochem **74**, 283-293.

Zalabak D, Johnova P, Plihal O, Senkova K, Samajova O, Jiskrova E, Novak O, Jackson D, Mohanty A, Galuszka P. 2016. Maize cytokinin dehydrogenase isozymes are localized predominantly to the vacuoles. Plant Physiol Biochem **104**, 114-124.

Zalewski W, Galuszka P, Gasparis S, Orczyk W, Nadolska-Orczyk A. 2010. Silencing of the HvCKX1 gene decreases the cytokinin oxidase/dehydrogenase level in barley and leads to higher plant productivity. J Exp Bot **61**, 1839-1851.

Zhang L, Zhao YL, Gao LF, Zhao GY, Zhou RH, Zhang BS, Jia JZ. 2012. TaCKX6-D1, the ortholog of rice OsCKX2, is associated with grain weight in hexaploid wheat. New Phytol **195**, 574-584.

Zhang W, Peng KX, Cui FB, Wang DL, Zhao JZ, Zhang YJ, Yu NN, Wang YY, Zeng DL, Wang YH, Cheng ZK, Zhang KW. 2021. Cytokinin oxidase/dehydrogenase OsCKX11 coordinates source and sink relationship in rice by simultaneous regulation of leaf senescence and grain number. Plant Biotechnol J **19**, 335-350.

FIGURE LEGENDS

Figure 1. Genetic relationship and expression patterns of *OsCKX* genes based on RNA sequencing data and GUS staining assay.

(A) Genetic relationship and expression patterns of *OsCKX* genes investigated in the leaf blade at the vegetative stage (LBV), leaf sheath at the vegetative stage (LSV), root at the vegetative stage (RV), leaf blade at the reproductive stage (LBR), leaf sheath at the reproductive stage (LSR), root at the reproductive stage (RR), stem (S), inflorescence meristem (IM), flower (F), and grain (G). The expression pattern was based on $\log_2$ (Fragments Per Kilobase of exon model per Million mapped fragments (FPKM) +1) values. **(B)** Histochemical GUS staining of *pOsCKX::GUS* transgenic plants at various developmental stages. The scale bar in B was 1 mm.

Figure 2. Phenotypic characterization of Nipponbare (NIP) and *osckx1/2* plants in 2021.

(A) Panicle phenotypes of NIP and *osckx1/2* mutants. The image was digitally extracted and scaled for comparison (scale bar = 10 cm). **(B–G)** Measurement of the primary branches per panicle (B), secondary branches per panicle (C), spikelets per panicle (D), seed setting rate (E), panicles per plant (F) and yield per plant (G) of NIP and *osckx1/2* mutants (n > 30 for B–E, n > 15 for F and G). P values indicate the significant differences between NIP and *osckx1/2* mutants determined using the Student's *t*-test.

Figure 3. Phenotypic characterization between Nipponbare (NIP) and *osckx4, osckx9,* and *osckx4/9* mutant plants from the field experiment.

(A) Phenotypic features of NIP, *osckx4*, *osckx9* and *osckx4/9* seedlings at the vegetative stage 46 days after sowing. The image was digitally extracted and scaled for comparison (scale bar = 10 cm). **(B, C)** Number of tillers at the vegetative stage 46 days after sowing (B) and reproductive stage 70 days after sowing (C) (n > 20

for NIP, *osckx4-6*, and *osckx9-1*, n = 10 for *osckx4/9*). **(D, E)** Habits (D) and panicle phenotypes (E) of NIP, *osckx4-6*, *osckx9-1*, and *osckx4/9* plants at the mature stage. The image was digitally extracted and scaled for comparison (scale bar = 10 cm). **(F–N)** Measurement of the panicle number (F), spikelets per panicle (G), primary branches per panicle (H), secondary branches per panicle (I), seed setting rate (J), 1,000-grain weight (K), yield per plant (L), diameter of basal internode (M), and plant height (N) of NIP, *osckx4-6*, *osckx9-1* (n > 20 for F–H and J–N, n = 5 for I), and *osckx4/9* (n > 10 for F–J and L–N, n = 5 for K). Different capital letters represent significant differences ($P < 0.01$) determined using one-way ANOVA and shortest significant ranges (SSR) test.

Figure 4. Phenotypic characterization between Nipponbare (NIP) and *osckx4*, *osckx9*, and *osckx4/9* mutant plants from the hydroponic experiment.

(A) Phenotypic features of Nipponbare (NIP), *osckx4*, *osckx9*, and *osckx4/9* seedlings 21 days after transferring to hydroponic solutions. The image was digitally extracted and scaled for comparison (scale bar = 10 cm). **(B–E)** Measurement of the shoot (above X axis) and root (below X axis) lengths (B), tiller numbers (C), length of 8th leaf (D), and width of 8th leaf (E) of NIP, *osckx4-6*, *osckx9-1*, and *osckx4/9* seedlings at 21 days after transplant (n = 24 each). Different capital letters represent significant differences ($P < 0.01$) determined using one-way ANOVA and SSR test.

Figure 5. RNA-seq analysis of the roots and shoot bases (BP) between Nipponbare (NIP) and *osckx4*, *osckx9*, and *osckx4/9* mutant plants.

(A) The number of differentially expressed genes (DEGs) identified in the roots and shoot bases of the following pairwise comparisons: Nipponbare (NIP) vs. *osckx4*, NIP vs. *osckx9*, and NIP vs. *osckx4/9*. The changes in gene

expression levels were calculated using the $\log_2$ fold change and *Q* values from three biological replicates. **(B)** Overlapping DEGs in the roots and shoot bases (BP) of NIP vs. *osckx4*, NIP vs. *osckx9*, and NIP vs. *osckx4/9*. **(C)** DEGs in *osckx4* and *osckx9* specifically and in common in the roots and shoots, genes in magenta are upregulated; genes in sky blue are downregulated. **(D)** Top enriched Kyoto Encyclopedia of Genes and Genomes (KEGG) pathways of the DEGs identified in the roots and shoot bases of NIP vs. *osckx4/9*.

Figure 6. OsCKX4 and OsCKX9 can regulate endogenous cytokinin levels in plant tissues.

(A) Differentially expressed type-A *OsRR* genes in the root (R) and shoot base (BP) of different mutants compared with Nipponbare (NIP). The fold change was based on $\log_2$ ($FPKM_{mutant}/FPKM_{NIP}$) values. * $Q < 0.05$, ** $Q < 0.01$. **(B)** Transcript levels of *OsRR* genes at 0–1 cm axillary buds determined using qRT-PCR. β-Actin was used as a reference gene. Results are presented relative to NIP. Data represent means ± SD (n = 3). P values represent significant difference between NIP and *osckx4/9*. * $P < 0.05$, ** $P < 0.01$, determined using the student's *t*-test. **(C, D)** The content of endogenous cytokinins in root (C) and shoot base (D) of 4-week-old seedlings. Data represent means ± SD (n = 4). P values indicate the significant differences between NIP and *osckx4/9* mutants determined using the Student's *t*-test.

Figure 7. OsCKX4 and OsCKX9 are associated with strigolactone biosynthesis and signaling transduction.

(A) Differentially expressed genes (DEGs) related to strigolactone metabolism and signaling transduction in the root (R) and shoot base (BP) of different mutants compared with Nipponbare (NIP). The fold change was based on $\log_2$ ($FPKM_{mutant}/FPKM_{WT}$) values. * $Q < 0.05$, ** $Q < 0.01$. **(B)** Transcript levels of genes related to strigolactone metabolism and signaling transduction at 0–1 cm axillary buds determined using qRT-PCR. β-Actin was used as a reference gene. Results are presented relative to NIP. Data represent means ± SD (n = 3). P values

represent significant difference between NIP and *osckx4/9*. * $P < 0.05$, ** $P < 0.01$, determined using the Student's *t*-test.

Figure 8. OsCKX4 and OsCKX9 are associated with gibberellin metabolism and signaling transduction.

Differentially expressed genes (DEGs) related to gibberellin metabolism and signaling transduction in the root (R) and shoot base (BP) of different mutants compared with Nipponbare (NIP). The fold change was based on $\log_2 (FPKM_{mutant}/FPKM_{WT})$ values. * $Q < 0.05$, ** $Q < 0.01$.

Figure 9. Functions of *OsCKX* genes in rice.

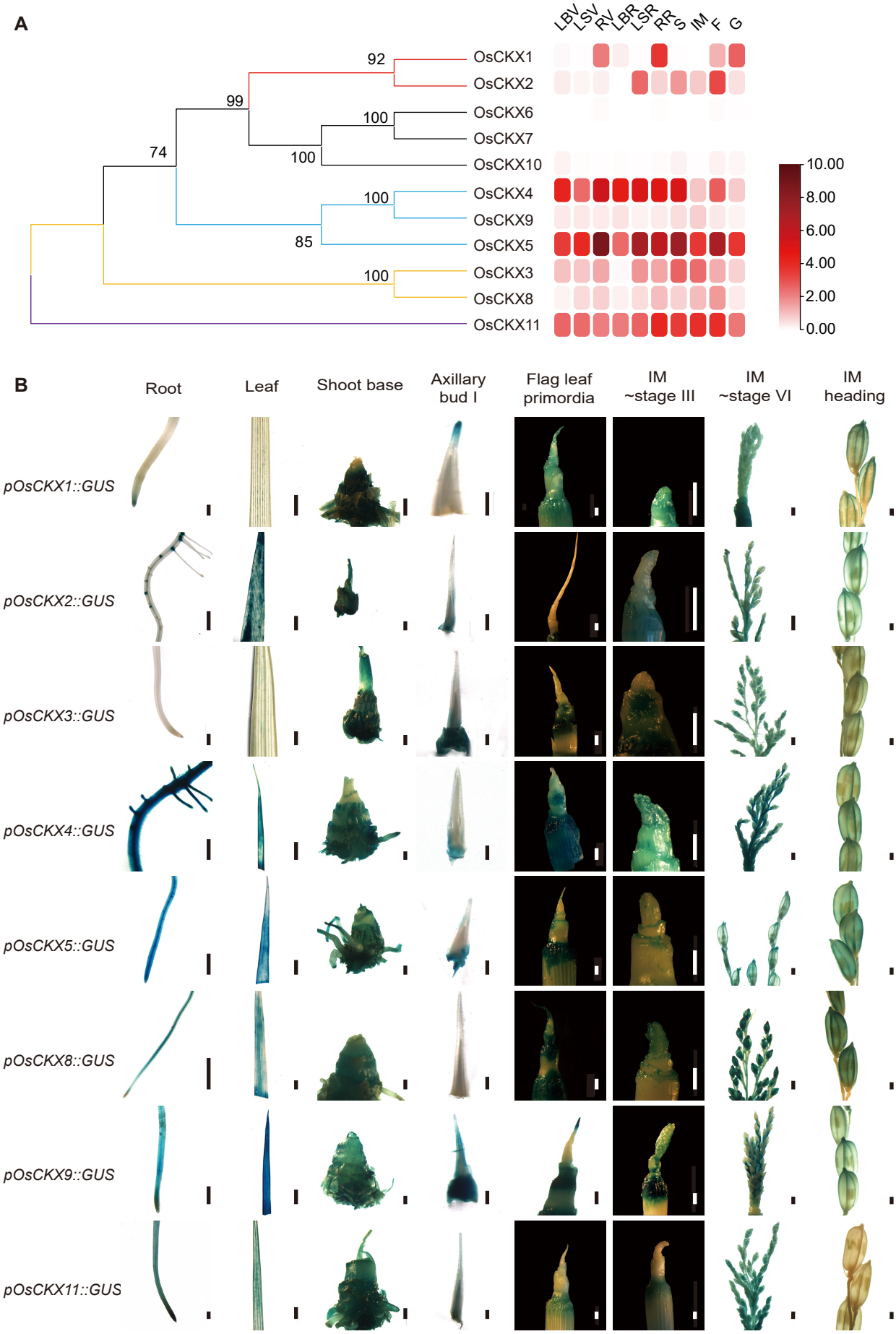

Figure 1. Genetic relationship and expression patterns of *OsCKX* genes based on RNA sequencing data and GUS staining assay.

A, Genetic relationship and expression patterns of *OsCKX* genes investigated in the leaf blade at the vegetative stage (LBV), leaf sheath at the vegetative stage (LSV), root at the vegetative stage (RV), leaf blade at the reproductive stage (LBR), leaf sheath at the reproductive stage (LSR), root at the reproductive stage (RR), stem (S), inflorescence meristem (IM), flower (F), and grain (G). The expression pattern was based on $\log_2$ (Fragments Per Kilobase of exon model per Million mapped fragments (FPKM) +1) values. B, Histochemical GUS staining of *pOsCKX::GUS* transgenic plants at various developmental stages. The scale bar in B was 1 mm.

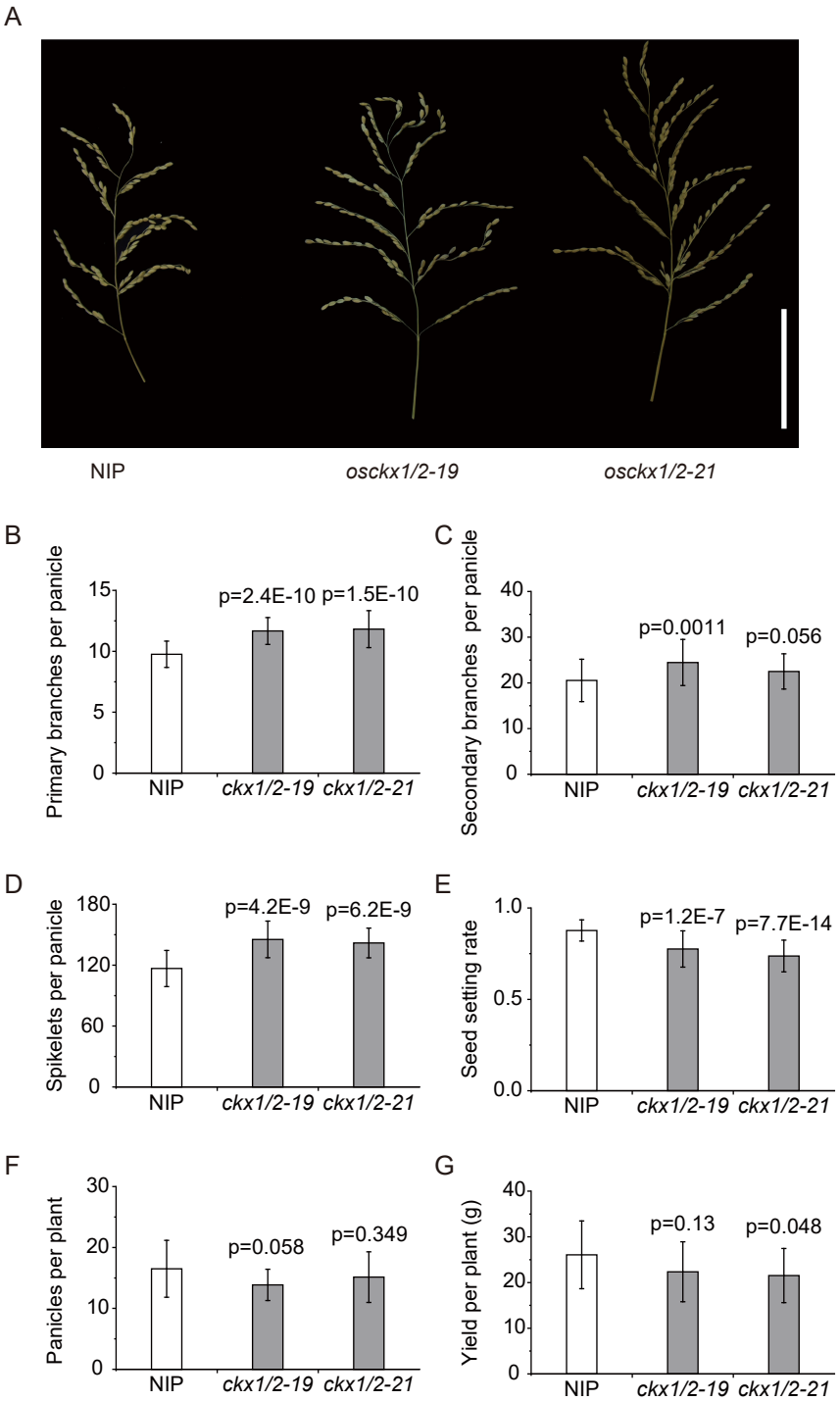

Figure 2. Phenotypic characterization of Nipponbare (NIP) and *osckx1/2* plants in 2021.
(A) Panicle phenotypes of NIP and *osckx1/2* mutants. The image was digitally extracted and scaled for comparison (scale bar = 10 cm). (B–G) Measurement of the primary branches per panicle (B), secondary branches per panicle (C), spikelets per panicle (D), seed setting rate (E), panicles per plant (F) and yield per plant (G) of NIP and *osckx1/2* mutants (n > 30 for B–E, n > 15 for F and G). P values indicate the significant differences between NIP and *osckx1/2* mutants determined using the Student's *t*-test.

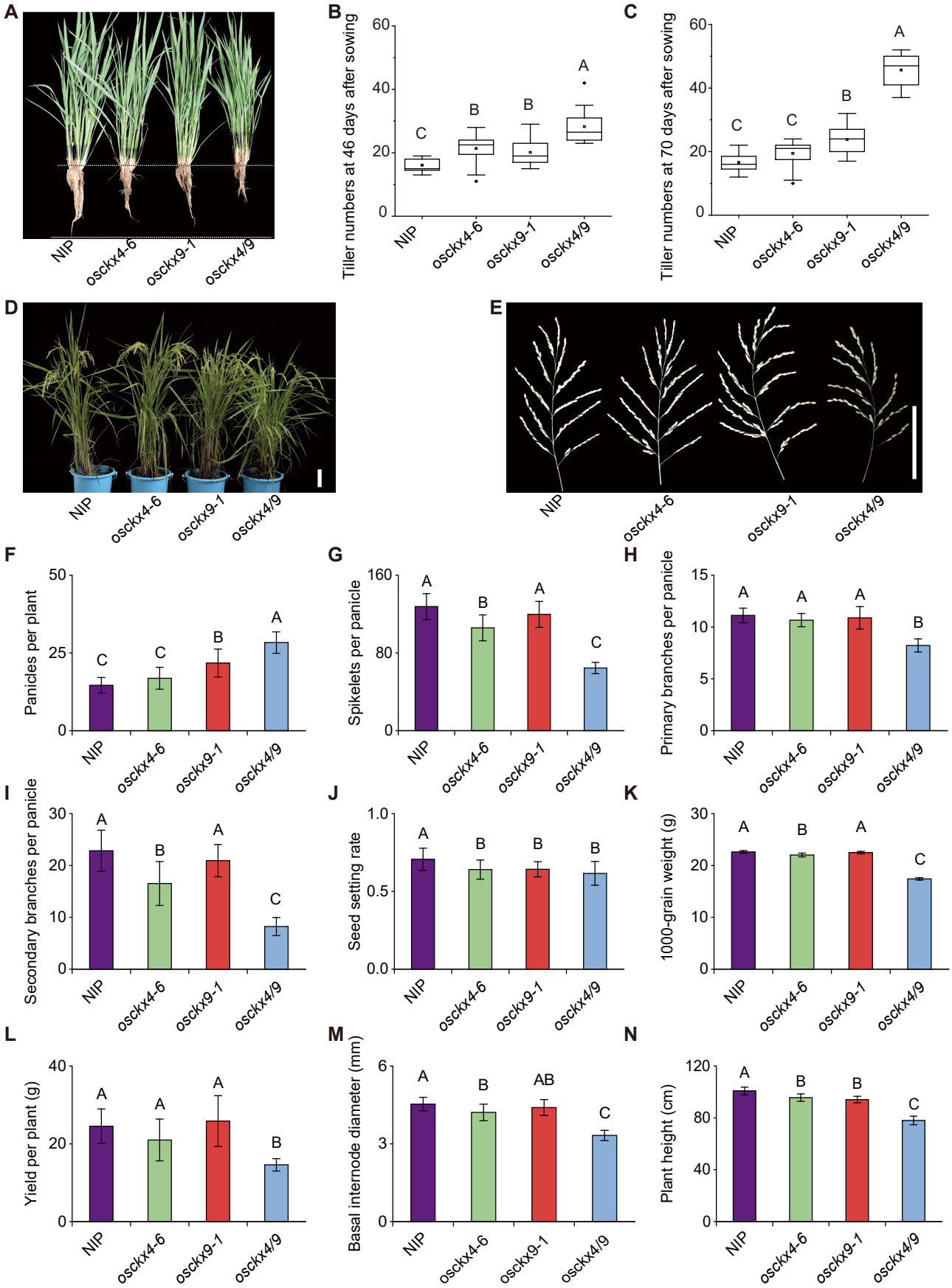

Figure 3. Phenotypic characterization between Nipponbare (NIP) and *osckx4*, *osckx9*, and *osckx4/9* mutant plants from the field experiment.

(A) Phenotypic features of NIP, *osckx4*, *osckx9* and *osckx4/9* seedlings at the vegetative stage 46 days after sowing. The image was digitally extracted and scaled for comparison (scale bar = 10 cm). **(B, C)** Number of tillers at the vegetative stage 46 days after sowing (B) and reproductive stage 70 days after sowing (C) (n > 20 for NIP, *osckx4-6*, and *osckx9-1*, n = 10 for *osckx4/9*). **(D, E)** Habits (D) and panicle phenotypes (E) of NIP, *osckx4-6*, *osckx9-1*, and *osckx4/9* plants at the mature stage. The image was digitally extracted and scaled for comparison (scale bar = 10 cm). **(F–N)** Measurement of the panicle number (F), spikelets per panicle (G), primary branches per panicle (H), secondary branches per panicle (I), seed setting rate (J), 1,000-grain weight (K), yield per plant (L), diameter of basal internode (M), and plant height (N) of NIP, *osckx4-6*, *osckx9-1* (n > 20 for F–H and J–N, n = 5 for I), and *osckx4/9* (n > 10 for F–J and L–N, n = 5 for K). Different capital letters represent significant differences (P < 0.01) determined using one-way ANOVA and shortest significant ranges (SSR) test.

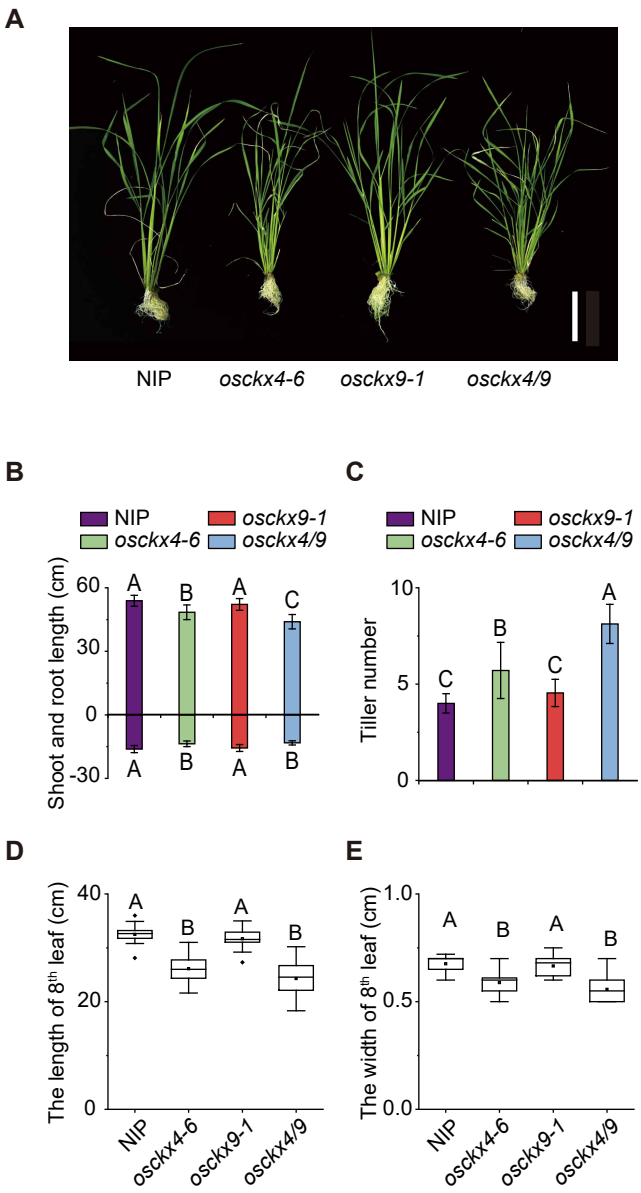

Figure 4. Phenotypic characterization between Nipponbare (NIP) and *osckx4*, *osckx9*, and *osckx4/9* mutant plants from the hydroponic experiment.
(A) Phenotypic features of Nipponbare (NIP), *osckx4-6*, *osckx9-1*, and *osckx4/9* seedlings 21 days after transferring to hydroponic solutions. The image was digitally extracted and scaled for comparison (scale bar = 10 cm). (B–E) Measurement of the shoot (above X axis) and root (below X axis) lengths (B), tiller numbers (C), length of 8th leaf (D), and width of 8th leaf (E) of NIP, *osckx4-6*, *osckx9-1*, and *osckx4/9* seedlings at 21 days after transplant (n = 24 each). Different capital letters represent significant differences ($P < 0.01$) determined using one-way ANOVA and SSR test.

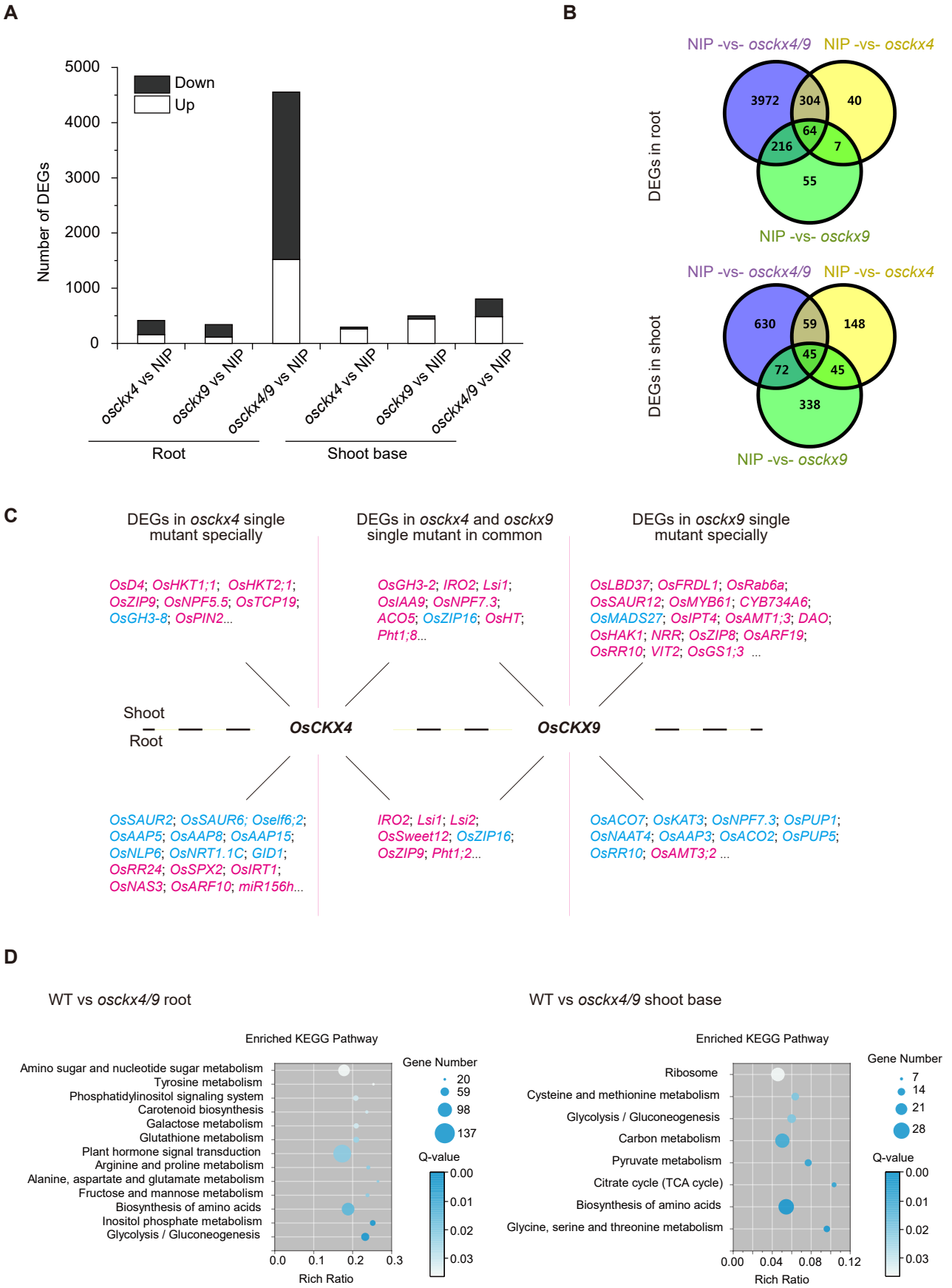

Figure 5. RNA-seq analysis of the roots and shoot bases (BP) between Nipponbare (NIP) and *osckx4*, *osckx9*, and *osckx4/9* mutant plants.
(A) The number of differentially expressed genes (DEGs) identified in the roots and shoot bases of the following pairwise comparisons: NIP vs. *osckx4*, NIP vs. *osckx9*, and NIP vs. *osckx4/9*. The changes in gene expression levels were calculated using the $\log_2$ fold change and Q values from three biological replicates. **(B)** Overlapping DEGs in the roots and shoot bases (BP) of NIP vs. *osckx4*, NIP vs. *osckx9*, and NIP vs. *osckx4/9*. **(C)** DEGs in *osckx4* and *osckx9* specifically and in common in the roots and shoots, genes in magenta are upregulated; genes in sky blue are downregulated. **(D)** Top enriched Kyoto Encyclopedia of Genes and Genomes (KEGG) pathways of the DEGs identified in the roots and shoot bases of NIP vs. *osckx4/9*.

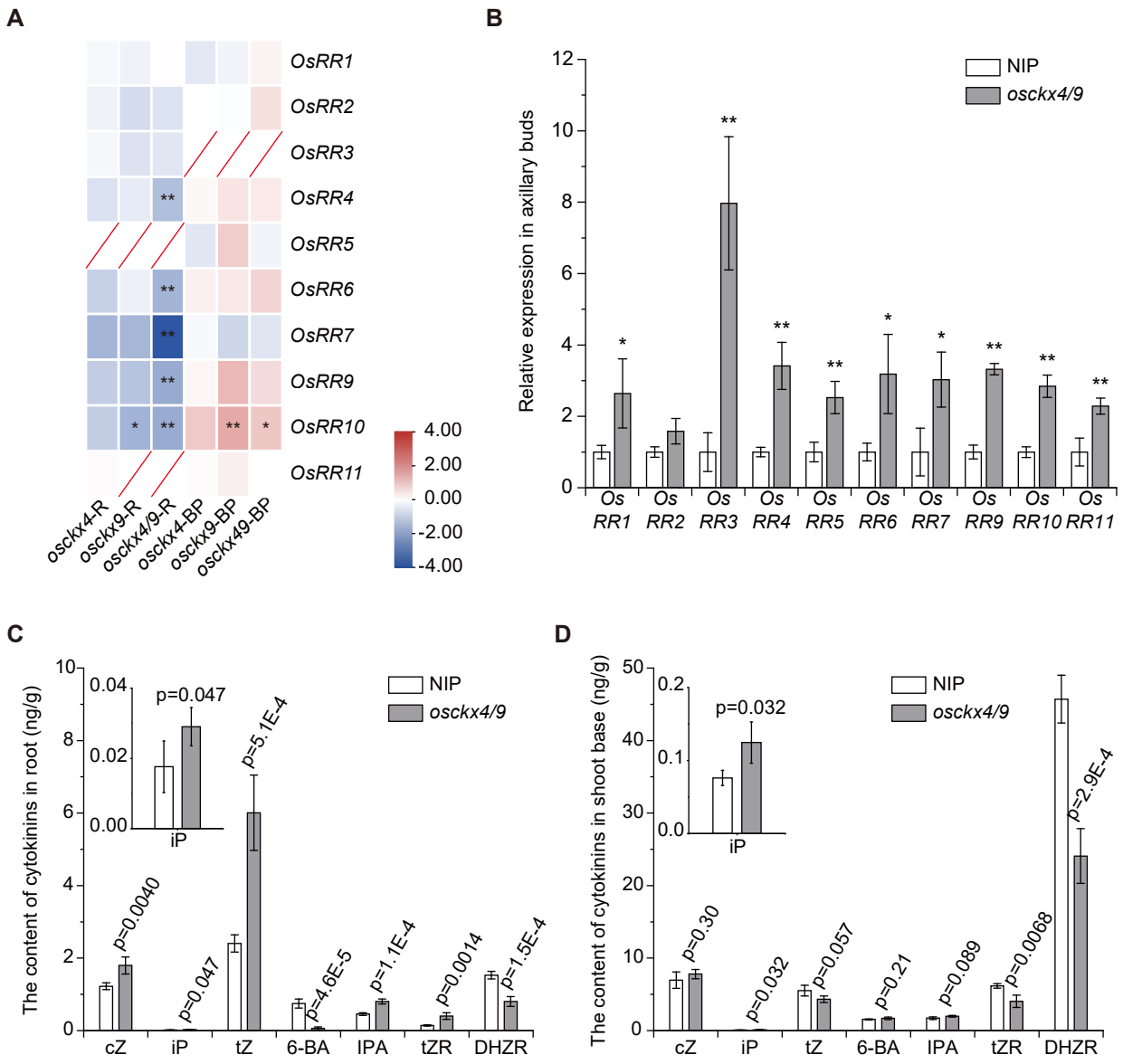

Figure 6. OsCKX4 and OsCKX9 can regulate endogenous cytokinin levels in plant tissues.
(A) Differentially expressed type-A *OsRR* genes in the root (R) and shoot base (BP) of different mutants compared with Nipponbare (NIP). The fold change was based on $\log_2$ ($FPKM_{mutant}/FPKM_{NIP}$) values. * Q < 0.05, ** Q < 0.01. (B) Transcript levels of *OsRR* genes at 0–1 cm axillary buds determined using qRT-PCR. β-Actin was used as a reference gene. Results are presented relative to NIP. Data represent means ± SD (n = 3). P values represent significant difference between NIP and *osckx4/9*. * P < 0.05, ** P < 0.01, determined using the student's t-test. (C, D) The content of endogenous cytokinins in root (C) and shoot base (D) of 4-week-old seedlings. Data represent means ± SD (n = 4). P values indicate the significant differences between NIP and *osckx4/9* mutants determined using the Student's *t*-test.

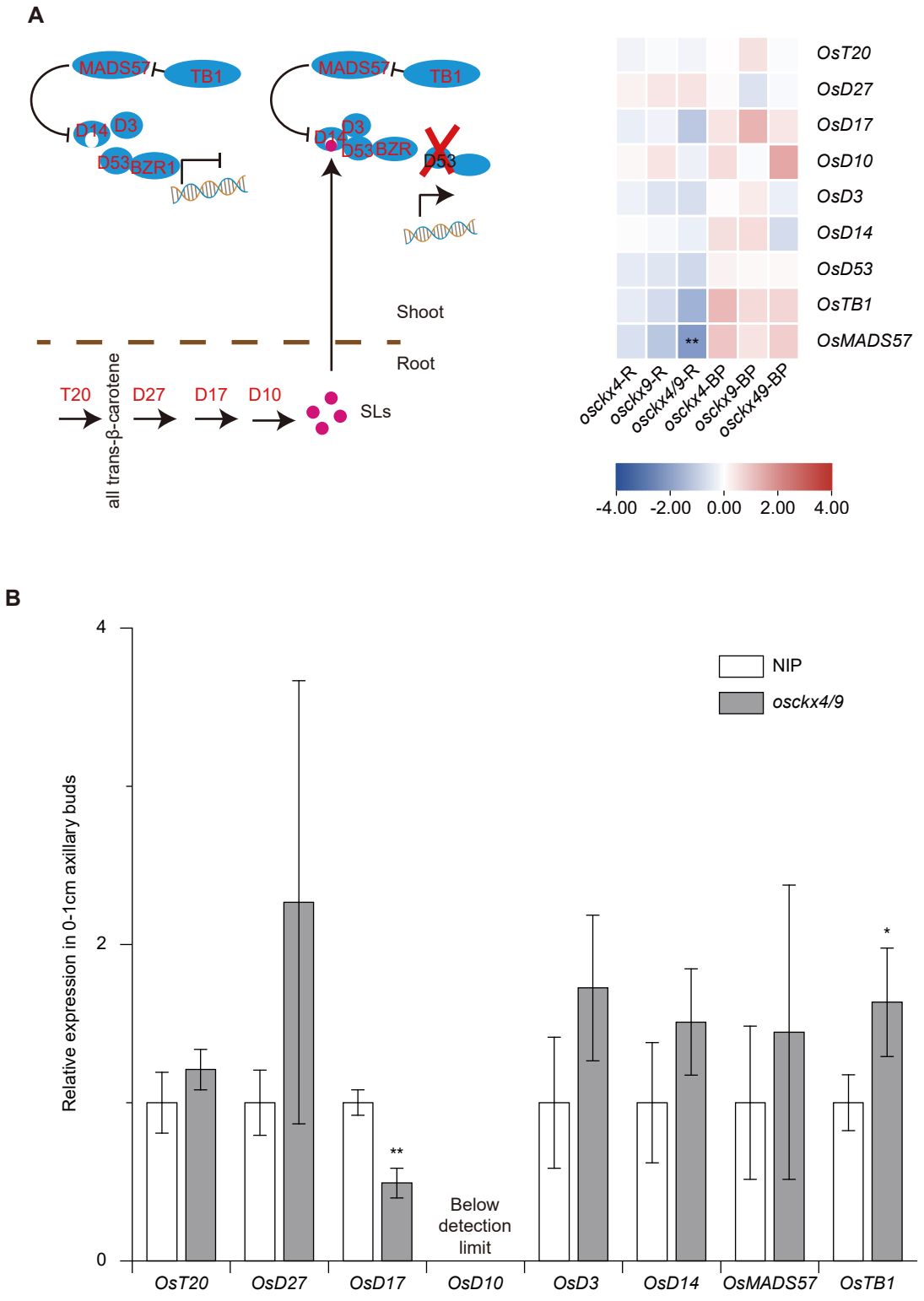

Figure 7. OsCKX4 and OsCKX9 are associated with strigolactone biosynthesis and signaling transduction

(A) Differentially expressed genes (DEGs) related to strigolactone metabolism and signaling transduction in the root (R) and shoot base (BP) of different mutants compared with Nipponbare (NIP). The fold change was based on $\log_2$ ($FPKM_{mutant}/FPKM_{WT}$) values. * Q < 0.05, ** Q < 0.01. (B) Transcript levels of genes related to strigolactone metabolism and signaling transduction at 0–1 cm axillary buds determined using qRT-PCR. β-Actin was used as a reference gene. Results are presented relative to NIP. Data represent means ± SD (n = 3). P values represent significant difference between NIP and *osckx4/9*. * P < 0.05, ** P < 0.01, determined using the Student's *t*-test.

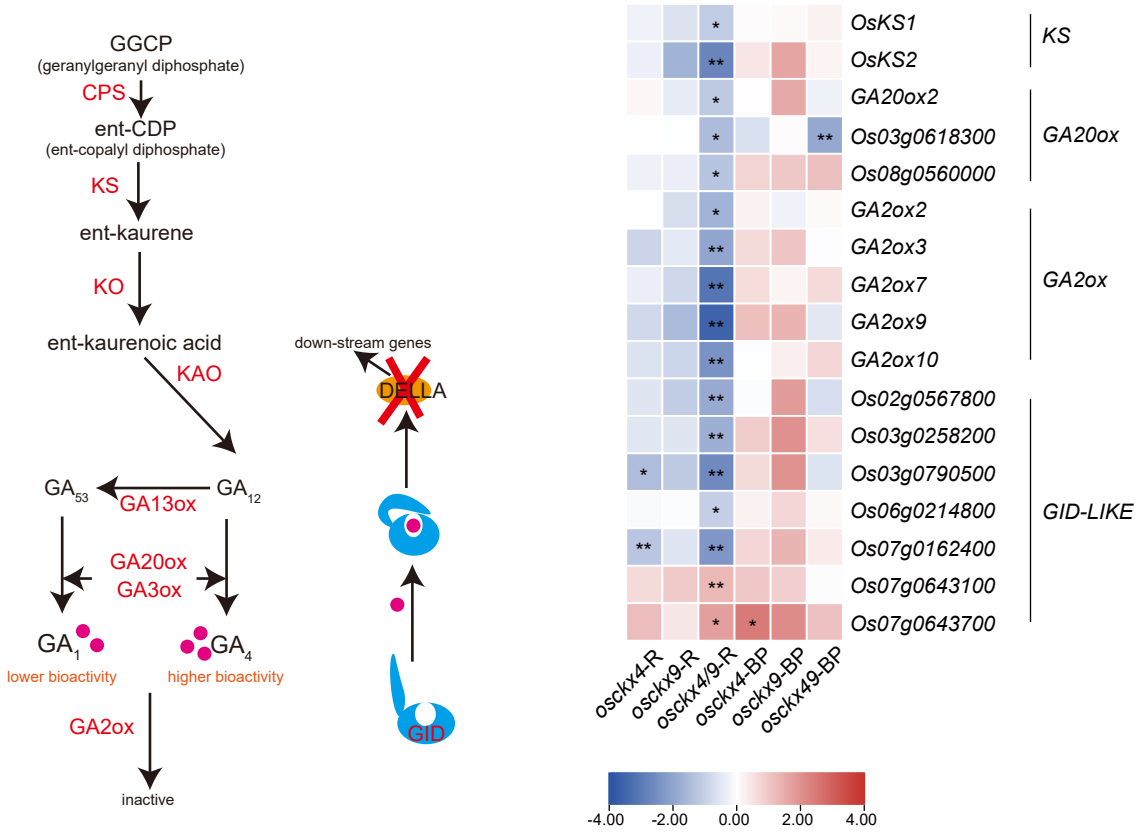

Figure 8. OsCKX4 and OsCKX9 are associated with gibberellin metabolism and signaling transduction

Differentially expressed genes (DEGs) related to gibberellin metabolism and signaling transduction in the root (R) and shoot base (BP) of different mutants compared with Nipponbare (NIP). The fold change was based on $\log_2$ ($FPKM_{mutant}/FPKM_{WT}$) values.* Q < 0.05, ** Q < 0.01.

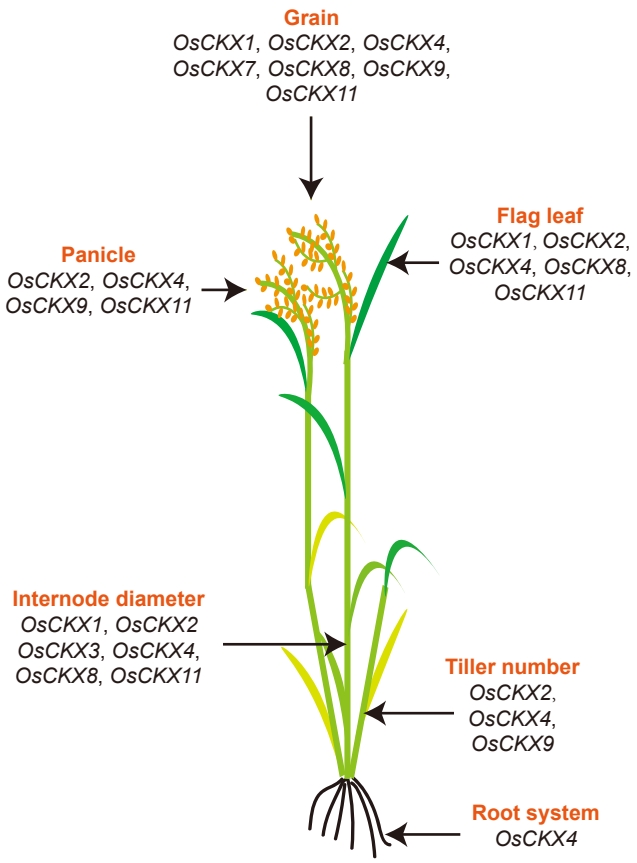

Figure 9. Functions of *OsCKX* genes in rice.